Journal of Hepatocellular Carcinoma

Dovepress
Taylor & Francis Group

Open Access Full Text Article

ORIGINAL RESEARCH

USP9X Promotes Hepatocellular Carcinoma Progression via Stabilization of HSP90AA1

Hanlin Jiang[1,*], Lining Huang[1,*], Jiahao Chen[1,*], Zongying Jiang[1], Weiqiao Niu[1], Jianwu Wu[1], Zhiming Qiao[1], Yujia Pan[2], Xinwei Jiang[1]

[1]Department of Hepatobiliary Surgery, The Affiliated Suzhou Hospital of Nanjing Medical University, Nanjing Medical University, Suzhou, People's Republic of China; [2]Center for Scientific Research and Innovation, The Affiliated Suzhou Hospital of Nanjing Medical University, Nanjing Medical University, Suzhou, People's Republic of China

*These authors contributed equally to this work

Correspondence: Xinwei Jiang, Department of Hepatobiliary Surgery, The Affiliated Suzhou Hospital of Nanjing Medical University, Nanjing Medical University, Suzhou, People's Republic of China, Email jxw19681022@163.com; Yujia Pan, Center for Scientific Research and Innovation, The Affiliated Suzhou Hospital of Nanjing Medical University, Nanjing Medical University, Suzhou, People's Republic of China, Email pyjseven@sina.com

Background: Hepatocellular carcinoma (HCC) is a leading cause of cancer-related mortality worldwide. Ubiquitin-specific proteases (USPs) modulate tumor progression by regulating substrate protein stability. However, the mechanisms of most DUBs in HCC remain poorly understood. This study aimed to investigate the role of USP9X in promoting HCC cell proliferation, survival, migration, and invasion.

Methods: Transcriptomic and clinical data of LIHC patients were obtained from TCGA to assess USP9X expression, prognosis, and pathway enrichment. USP9X expression in HCC and adjacent tissues was examined by immunohistochemistry and Western blotting. Functional assays (CCK-8, colony formation, wound-healing, Transwell) were performed following USP9X knockdown or overexpression in Lm3 and Huh7 cells. The USP9X–HSP90AA1 interaction was evaluated by Co-IP and mass spectrometry, and deubiquitination assays elucidated the mechanism. In vitro and in vivo experiments determined the effects of USP9X–HSP90AA1 signaling on HCC growth and metastasis.

Results: Bioinformatic analyses revealed that USP9X expression was significantly elevated in LIHC tissues and correlated with poor prognosis. Immunohistochemistry and Western blotting confirmed higher USP9X protein levels in tumor tissues. Knockdown of USP9X inhibited proliferation and migration of Lm3 and Huh7 cells, whereas USP9X overexpression enhanced these phenotypes. Co-IP demonstrated a direct interaction between USP9X and HSP90AA1, and deubiquitination assays showed that USP9X decreased HSP90AA1 ubiquitination and increased its stability. Both in vitro and in vivo data indicated that USP9X promotes HCC progression through stabilization of HSP90AA1.

Conclusion: USP9X is a tumor-promoting factor that accelerates HCC progression by stabilizing HSP90AA1, highlighting USP9X as a potential therapeutic target for HCC.

Keywords: HCC, USP9X, HSP90AA1, deubiquitination, CO-IP, bioinformatics translation

Introduction

Primary liver cancer remains a major global health burden, ranking as the sixth most commonly diagnosed malignancy and the third leading cause of cancer-related death worldwide, with a substantial and persistent disease burden across regions.[1,2] According to GLOBOCAN 2022, liver cancer accounted for 865,269 new cases and 757,948 deaths globally in 2022. China bears a particularly heavy burden, with 367,700 new cases and 316,500 deaths in 2022, accounting for 42.5% of global incident cases. In the United States, liver and intrahepatic bile duct cancer is projected to cause 42,340 new cases and 30,980 deaths in 2026.[1,3–6] Although novel biomarkers such as Glypican-3 and Dickkopf-1 have been introduced into clinical practice,[7,8] and the 5-year survival rate of patients with early-stage hepatocellular carcinoma (HCC) can reach 70% following curative resection or liver transplantation,[9] postoperative recurrence remains alarmingly

https://doi.org/10.2147/JHC.S585217
Received: 28 November 2025
Accepted: 5 May 2026
Published: 12 May 2026

high—around 15% after transplantation and up to 60% after partial hepatectomy.[10,11] The 5-year survival rate for recurrent cases drops to 20–35%,[12] with most relapses occurring intrahepatically, indicating a persistently tumor-promoting hepatic microenvironment.[13] Moreover, the pronounced heterogeneity of HCC leads to unpredictable therapeutic responses and variable clinical outcomes.[14] Therefore, elucidating the molecular mechanisms underlying HCC initiation and progression remains an urgent and critical challenge.

In eukaryotic cells, protein homeostasis (proteostasis) is essential for maintaining cellular function and regulating development and aging. This homeostatic network comprises coordinated molecular processes that preserve proteome integrity; its disruption contributes to metabolic disorders, tumorigenesis, neurodegeneration, and cardiovascular disease.[15] Within this system, the ubiquitin–proteasome pathway (UPP) plays a central role in regulating protein turnover and quality control.[16] Ubiquitin ligases (E3s) catalyze the attachment of ubiquitin chains to substrate proteins, marking them for degradation or functional modification, while deubiquitinating enzymes (DUBs) remove or remodel these ubiquitin tags to stabilize proteins and fine-tune signaling activity. These opposing processes precisely regulate key pathways such as p53, PI3K–AKT, DNA repair, metabolism, and immune checkpoint signaling. Disruption of this balance leads to proteostatic collapse, driving oncogenesis, metastasis, and therapeutic resistance.[17–19]

Several DUBs have been implicated in HCC pathogenesis and metastasis.[20] Among them, USP9X is a prominent member of the USP family that regulates numerous biological processes—including cell-cycle progression, mitosis, intracellular transport, epithelial–mesenchymal transition, apoptosis resistance, immune modulation, stemness, and drug tolerance—mainly by stabilizing substrate proteins. USP9X expression and activity are further modulated by non-coding RNAs.[21] Functionally, USP9X exhibits context-dependent roles in tumorigenesis: it is aberrantly expressed in acute myeloid leukemia,[22] lung cancer,[23] pancreatic cancer,[24] and glioblastoma,[25] often acting as an oncogene, while in certain malignancies it may exert tumor-suppressive functions.[26] However, the precise role and prognostic significance of USP9X in HCC remain insufficiently characterized, making it an attractive target for mechanistic and therapeutic exploration.

Heat shock proteins (HSPs) are frequently upregulated in tumors and closely associated with therapeutic resistance. In HCC, HSPs promote tumor progression by sustaining cell survival, enhancing drug resistance, and facilitating metastasis, thereby serving as key biomarkers for diagnosis, prognosis, and therapy.[27,28] HSP90AA1, a major cytosolic isoform of the HSP90 family, functions as a critical molecular chaperone and potential therapeutic target in cancer.[29] Recent studies show that HSP90AA1 can also be secreted extracellularly and interact with various client proteins—including oncogenic and signaling molecules—to drive tumor progression and invasion.[30–32] For instance, in HCC, FBXL6 binds to HSP90AA1 to stabilize and activate c-MYC, thereby promoting tumorigenesis.[33] Notably, the stability of HSP90AA1 is regulated by deubiquitinating enzymes;[34] however, whether USP9X modulates HSP90AA1 stability in HCC remains unknown.

In this study, we demonstrate that USP9X is markedly upregulated in HCC and correlates with poor prognosis. Functional assays reveal that USP9X promotes HCC malignancy both in vitro and in vivo by deubiquitinating and stabilizing HSP90AA1. Collectively, our findings establish USP9X as a tumor-promoting factor that facilitates HCC progression through HSP90AA1 stabilization, providing a theoretical foundation for developing USP9X-targeted therapeutic strategies.

Materials and Methods

Data Acquisition and Processing

Transcriptomic and clinical data of patients with liver hepatocellular carcinoma (LIHC) were retrieved from The Cancer Genome Atlas (TCGA) database. Clinical variables included age, sex, histological grade, pathological stage, pathological T stage, pathological N stage, survival time, and survival status. All bioinformatic analyses were performed in R software (version 4.5.1) using the TCGAbiolinks package (version 2.38.0), dplyr package (version 1.2.1), tidyverse package (version 2.0.0), and DESeq2 package (version 1.50.2). Raw count data were used for differential expression analysis with DESeq2, and P values were adjusted using the Benjamini–Hochberg method. Genes with $|\log_2$ fold change$| > 1$ and adjusted $P < 1 \times 10^{-6}$ were considered significantly differentially expressed. For expression visualization, gene

expression values were normalized and presented as transcripts per million (TPM). Gene set enrichment analysis (GSEA) was performed to identify activated pathways in LIHC, which revealed significant enrichment of the "protein ubiquitination" pathway based on the Reactome database. A Venn diagram was generated to identify the overlap between DEGs and members of the ubiquitin-specific peptidase (USP) family, yielding five candidate genes, including USP9X. Survival analysis and univariate Cox regression analysis were subsequently performed to evaluate their prognostic significance. Pan-cancer expression patterns were visualized using the TCGAplot package, and time-dependent receiver operating characteristic (ROC) curves were generated to assess the prognostic predictive value of USP9X. In addition, box plots were used to illustrate USP9X expression across different clinical stages.

Immunohistochemistry

Tumor and adjacent non-tumorous tissues were collected from 13 patients with pathologically confirmed hepatocellular carcinoma undergoing surgical resection at the Affiliated Suzhou Hospital of Nanjing Medical University. Paired paraffin-embedded tissue samples were used for qualitative immunohistochemical analysis of USP9X expression. None of the patients had received preoperative anticancer therapy. The study was conducted in accordance with the Declaration of Helsinki and approved by the Ethics Committee of the Affiliated Suzhou Hospital of Nanjing Medical University. Written informed consent was obtained from all participants.

IHC staining was performed as previously described,[35] using a PV-9000 detection kit (Zhongshan Golden Bridge, China). Briefly, 5-μm sections were baked at 60 °C for 2 h, deparaffinized in xylene, and rehydrated through graded ethanol. Antigen retrieval was performed by heating in citrate buffer at 98 °C for 15 min, followed by PBS washing. Endogenous peroxidase activity was blocked for 15 min, and nonspecific binding was blocked with 5% bovine serum albumin (BSA) for 30 min at 37 °C. Sections were then incubated overnight at 4 °C with primary anti-USP9X antibody (55054-1-AP, Proteintech, China; 1:100). After washing, slides were incubated with HRP-conjugated secondary antibody at 37 °C for 30 min, developed with DAB for 10 min, and counterstained with hematoxylin (G1120, Solarbio). Images were captured using an Olympus BX53 microscope, and IHC scores were quantified as previously reported.[36]

Cell Culture

Human HCC cell lines Lm3 and Huh7, as well as HEK293 cells, were obtained from the Cell Bank of the Chinese Academy of Sciences (Shanghai, China). All cell lines were authenticated by short tandem repeat (STR) profiling and confirmed to be free of mycoplasma contamination. Cells were cultured in Dulbecco's Modified Eagle Medium (DMEM; Gibco, China) supplemented with 10% fetal bovine serum (FBS) and 1% penicillin–streptomycin at 37 °C in a humidified incubator containing 5% CO_2.

RNA Extraction and Quantitative RT-PCR

Total RNA was extracted using TRIzol reagent (Invitrogen, USA), and reverse transcription was carried out according to the manufacturer's instructions. Quantitative real-time PCR (qRT-PCR) was performed using a 20 μL reaction containing gene-specific primers and SYBR Green master mix. Amplification and quantification were performed as previously described.[37] Relative mRNA expression levels were calculated using the $2^{-}\Delta\Delta Ct$ method. Primer sequences are listed in Supplementary Table 1.

siRNA, Plasmids, and Transfection

Small interfering RNAs (siRNAs) targeting USP9X and HSP90AA1 were synthesized by GenePharma (China); sequences are shown in Supplementary Table 2. Overexpression plasmids were obtained from TRANSHEEP BIO (China), with details provided in Supplementary Table 3. Lm3, Huh7, and HEK293 cells were seeded in 6-well plates (3×10^5 cells/well). When confluence reached ~70%, transfection was performed using Lipofectamine 3000 (Thermo Fisher Scientific, USA) following the manufacturer's protocol. USP9X and HSP90AA1 siRNAs or overexpression plasmids were introduced as indicated.

Western Blot Analysis

Western blotting was conducted as described previously. Briefly, total protein was extracted using RIPA buffer supplemented with protease inhibitors, quantified by BCA assay, and separated by SDS–PAGE, followed by transfer to PVDF membranes. Membranes were blocked with 5% BSA for 1 h at room temperature and incubated overnight at 4 °C with primary antibodies: anti-USP9X (55054-1-AP, Proteintech, China), anti-HSP90AA1 (60,318-1-Ig, Proteintech, China), and anti-β-tubulin (10068-1-AP, Proteintech, China) After washing, membranes were incubated with HRP-conjugated secondary antibodies, and signals were visualized using enhanced chemiluminescence (ECL). Band intensities were quantified using ImageJ software.

Functional Assays

Cell proliferation was assessed using the CCK-8 assay. Forty-eight hours after transfection, Lm3 and Huh7 cells were seeded in 96-well plates, and CCK-8 reagent (MCE, USA) was added following the manufacturer's instructions. Absorbance was measured at 450 nm using a BioTek microplate reader. For colony formation assays, 1×10^3 cells per well were seeded in 6-well plates and cultured for 7 days, fixed with methanol, and stained with 0.1% crystal violet. Colonies were counted under a light microscope. Transwell assays were used to assess migration and invasion. Cells were seeded in the upper chamber of Transwell inserts, with medium containing 20% FBS in the lower chamber as a chemoattractant. After 24 h of incubation at 37 °C, migrated cells were fixed, stained with 1% crystal violet, and counted in five random fields. For wound-healing assays, confluent monolayers were scratched using sterile 10 μL pipette tips. Images were taken at 0 h and 12 h to evaluate migration. All experiments were performed independently at least three times.

Animal Experiments

All animal experiments were approved by the Institutional Animal Care and Use Committee (IACUC) of Suzhou Institute of Systems Medicine. Animal care and use were performed in accordance with the welfare guidelines of the Animal Center of Suzhou Institute of Systems Medicine, based on AAALAC standards and Chinese regulations (GB/T 35892–2018). Four-week-old male BALB/c nude mice were obtained from GemPharmatech Co., Ltd. (Jiangsu, China) and randomly divided into four groups (n = 5 per group). Xenograft models were established by subcutaneous injection of Huh7 cells into the right axillary region. Rescue complexes containing siRNA, plasmid DNA, and Lipofectamine 3000 (1:1, v/v) were delivered by local intratumoral injection (20 μL per mouse). Tumor size was measured every 3 days, and tumor volume was calculated as $V = (\text{length} \times \text{width}^2)/2$. All procedures were conducted under isoflurane anesthesia (4% for induction and 1.5%–2.5% for maintenance). On day 18 after inoculation, mice were euthanized by CO_2 inhalation followed by cervical dislocation, and tumors were harvested and weighed. The endpoint at day 18 was chosen because it allowed sufficient tumor growth for meaningful comparison among groups while remaining within predefined humane endpoint limits.

Co-Immunoprecipitation (Co-IP) Assay

Cells were lysed in IP lysis buffer (R0100, Solarbio, China), and the supernatant was collected after centrifugation. Twenty microliters of protein A/G agarose beads (SC-2003, Santa Cruz Biotechnology, USA) were added and incubated at 4 °C for 30 min. Total protein concentrations were measured by BCA assay. Equal amounts of lysates were incubated overnight at 4 °C with the indicated primary antibodies and 60 μL of protein A/G beads. Beads were washed three times with IP lysis buffer, and bound proteins were eluted by boiling for 8 min at 99 °C, followed by Western blotting.

Ubiquitination Assay

HEK293 cells were co-transfected with plasmids encoding Flag-USP9X, HA-Ubiquitin, and Myc-HSP90AA1 or truncated/mutant forms of USP9X. After 24 h, cells were treated with 20 μM MG132 in DMEM for 6 h to inhibit proteasomal degradation. Cells were lysed in 200 μL SDS lysis buffer (ABS9117, Absin, China) and boiled for 8 min, then diluted with 0.8 mL IP lysis buffer. The supernatant was incubated with anti-Flag antibody and protein A/G beads

(SC-2003, Santa Cruz Biotechnology, USA) for 8 h at 4 °C. Beads were washed three times, eluted by boiling in loading buffer for 10 min, and analyzed by Western blot.

Statistical Analysis

Statistical analyses were performed using GraphPad Prism 9.0. Comparisons between two groups were made using unpaired *t*-tests, and multiple-group comparisons were conducted using one-way ANOVA. CCK-8 data were analyzed by two-way ANOVA. Survival curves were generated using the Kaplan–Meier method and compared by the Log rank test. Data are presented as mean ± standard deviation (SD). Statistical significance was defined as $P < 0.05$. All experiments were repeated independently at least three times.

Results

Identification of Prognostically Significant Ubiquitin-Specific Proteases in HCC

Transcriptomic and clinical data from hepatocellular carcinoma (TCGA-LIHC) patients were analyzed to identify differentially expressed genes (DEGs) and prognostic deubiquitinases (DUBs). A volcano plot revealed substantial expression differences between tumor and normal tissues, identifying 4053 DEGs—3046 upregulated and 1007 downregulated (Figure 1A). Gene set enrichment analysis (GSEA) using the Reactome database indicated significant activation of the "Protein ubiquitination" pathway in LIHC (Figure 1B). Intersecting DEGs with the Ubiquitin Specific Peptidase gene family yielded five candidates—USP9X, USP21, USP38, USP49, and USP54 (Figure 1C). Subsequent survival and univariate Cox analyses showed that USP9X was significantly associated with patient prognosis, while USP38, USP49, and USP54 lacked prognostic relevance (Figure 1D–I). Although USP21 also exhibited prognostic significance in the TCGA-LIHC dataset, previous studies provided limited protein-level and functional validation, reducing its predictive utility. In contrast, USP9X was consistently reported to be upregulated at both mRNA and protein levels and demonstrated clear oncogenic effects in vitro and in vivo.[38] Therefore, USP9X was selected for further mechanistic investigation as a potential key regulator of HCC progression.

USP9X is Upregulated in HCC and Correlates with Poor Prognosis and Advanced Tumor Stage

Pan-cancer expression analysis using the TCGAPlot package revealed markedly elevated USP9X expression across multiple tumor types compared with normal tissues (Figure 2A and B). Specifically, in HCC, violin plots and paired-sample comparisons confirmed significantly higher USP9X mRNA levels in tumor tissues than in normal liver tissues (Figure 2C and D). Receiver operating characteristic (ROC) analysis showed that USP9X expression had moderate predictive accuracy for 1-year overall survival (AUC = 0.624) (Figure 2E). Kaplan–Meier survival analysis further demonstrated that high USP9X expression was associated with shorter overall survival (HR = 1.45, P = 0.033) and progression-free intervals (HR = 1.43, P = 0.026) (Figure 2F and G). Moreover, USP9X expression was positively correlated with clinical stage ($P < 0.05$) (Figure 2H). Immunohistochemistry revealed stronger USP9X staining in tumor tissues compared with adjacent non-tumorous tissues (Figure 2I), and Western blot analysis of four paired samples confirmed elevated USP9X protein levels in tumors (Figure 2J). Collectively, these results provide consistent evidence that USP9X is significantly upregulated in HCC and associated with advanced disease stage and poor prognosis, supporting its role as a potential oncogenic driver and prognostic biomarker.

Knockdown of USP9X Suppresses HCC Cell Proliferation and Tumorigenicity

To explore the functional role of USP9X in HCC, loss-of-function assays were conducted using siRNA-mediated knockdown in Huh7 and Lm3 cells. qRT-PCR and Western blot analyses confirmed efficient USP9X depletion by two independent siRNAs (si-USP9X-1# and si-USP9X-2#) at both mRNA and protein levels (Figure 3A–F). CCK-8 assays showed that USP9X knockdown significantly inhibited proliferation in both cell lines (Figure 3G and H). Consistently, colony formation assays revealed a marked reduction in clonogenic capacity upon USP9X silencing (Figure 3I). Transwell assays demonstrated that USP9X depletion impaired migration and invasion (Figure 3J), while wound-

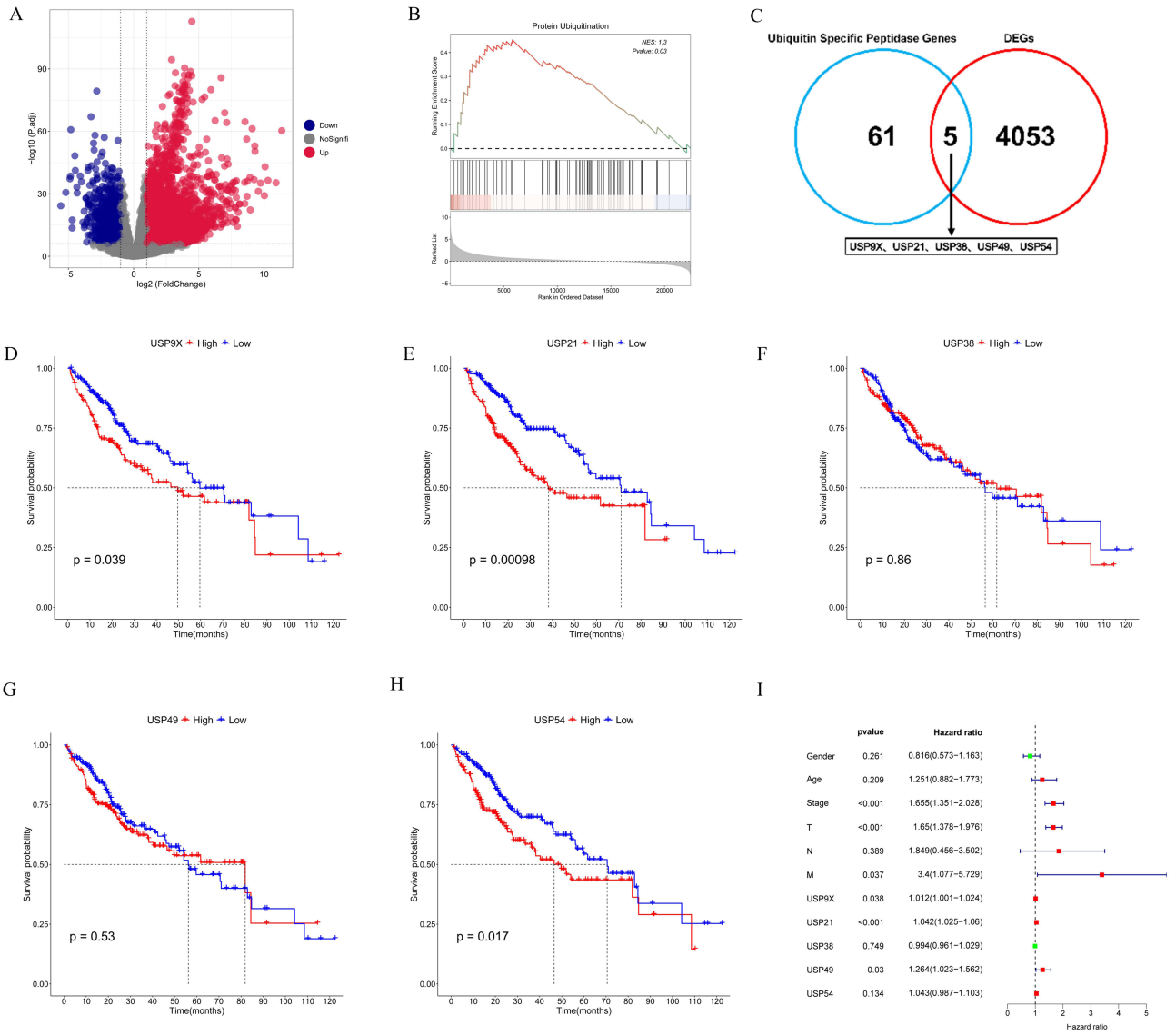

Figure 1 Identification of prognostically significant ubiquitin-specific proteases (USPs) in HCC. (**A**) Volcano plot showing differentially expressed genes (DEGs) between tumor and normal tissues; red dots represent upregulated genes, and blue dots represent downregulated genes. (**B**) Gene Set Enrichment Analysis (GSEA) reveals significant enrichment of the "Protein Ubiquitination" pathway in HCC (NES = 1.3, P = 0.03). (**C**) Venn diagram illustrating the overlap between DEGs and ubiquitin-specific peptidase (USP) family genes, identifying five candidates (USP9X, USP21, USP38, USP49, and USP54). (**D**–**H**) Kaplan–Meier survival curves comparing overall survival in patients with high versus low expression of the five candidate genes. High expression of (**D**) USP9X (P = 0.039), (**E**) USP21 (P = 0.00098), and (**H**) USP54 (P = 0.017) is significantly associated with poor prognosis. (**I**) Multivariate Cox regression forest plot evaluating clinical parameters and the five candidate USPs as independent prognostic factors for overall survival.

healing assays confirmed delayed closure (Figure 3K). In vivo, xenograft tumors derived from USP9X-silenced cells exhibited smaller volumes and lower weights compared with controls after 18 days (n = 5 mice per group, Figure 3L). Together, these findings indicate that USP9X promotes HCC cell proliferation, migration, and tumorigenic capacity.

Overexpression of USP9X Enhances HCC Cell Proliferation and Tumor Growth

Gain-of-function experiments were performed to further validate the oncogenic role of USP9X. Overexpression of USP9X in Huh7 and Lm3 cells was verified by qRT-PCR and Western blotting (Figures 4A–Figure 4F). CCK-8 assays demonstrated enhanced proliferation upon USP9X overexpression (Figures 4G and Figure 4H). Consistently, colony formation assays showed increased colony numbers in USP9X-overexpressing cells (Figure 4I and J). Transwell and wound-healing assays confirmed that USP9X overexpression enhanced cell migration and invasion (Figures 4K–N). In

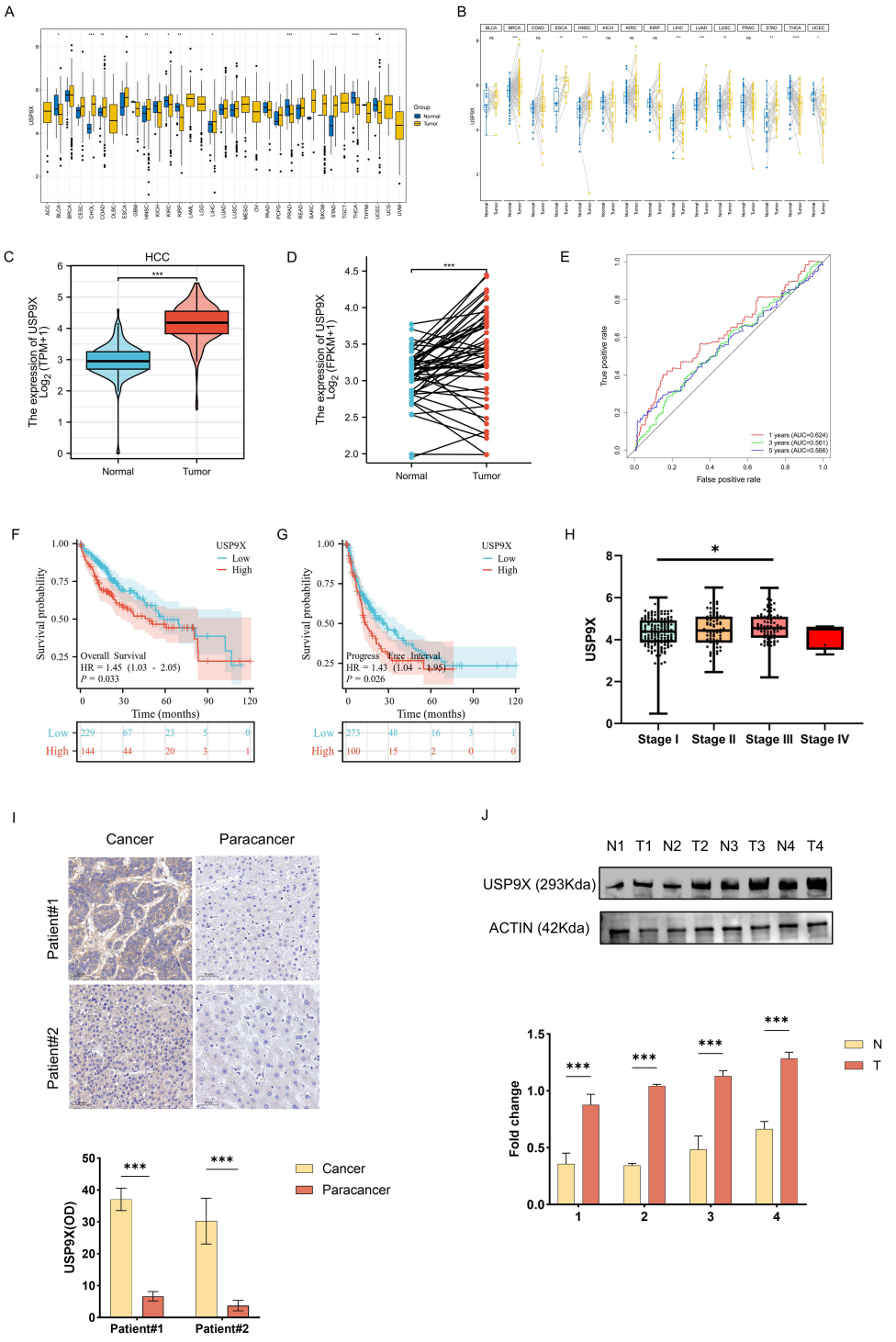

Figure 2 USP9X is upregulated in HCC and correlates with poor prognosis and malignant phenotypes. (**A**) Pan-cancer analysis of TCGA data showing that USP9X expression is significantly higher in multiple tumor types (yellow) compared to corresponding normal tissues (blue). (**B**) Paired-sample pan-cancer analysis confirming elevated USP9X expression in tumors. (**C** and **D**) TCGA-LIHC analysis showing significantly increased USP9X expression in HCC tissues versus adjacent normal tissues (P < 0.001), validated in paired samples (P < 0.001). (**E**) Receiver operating characteristic (ROC) curves evaluating the predictive value of USP9X expression for 1-, 3-, and 5-year survival (AUC = 0.624, 0.561, and 0.566, respectively). (**F** and **G**) Kaplan–Meier survival analyses showing that high USP9X expression predicts poorer (**F**) overall survival (HR = 1.45, P = 0.033) and (**G**) progression-free survival (HR = 1.43, P = 0.026). (**H**) USP9X expression in HCC tissues across different pathological stages. Boxplots show USP9X expression in stage I, stage II, stage III, and stage IV HCC, and the asterisk indicates a statistically significant difference among groups. (**I**) Representative immunohistochemistry (IHC) images showing stronger USP9X staining in tumor tissues compared with matched adjacent tissues from two HCC patients (Scale bar = 50 μm). (**J**) Western blot and quantitative analyses of four paired HCC samples confirming significantly higher USP9X protein levels in tumor (T) versus adjacent normal (N) tissues (*P < 0.05, **P < 0.01, ***P < 0.001, **** P < 0.0001, ns: not significant).

https://doi.org/10.2147/JHC.S585217

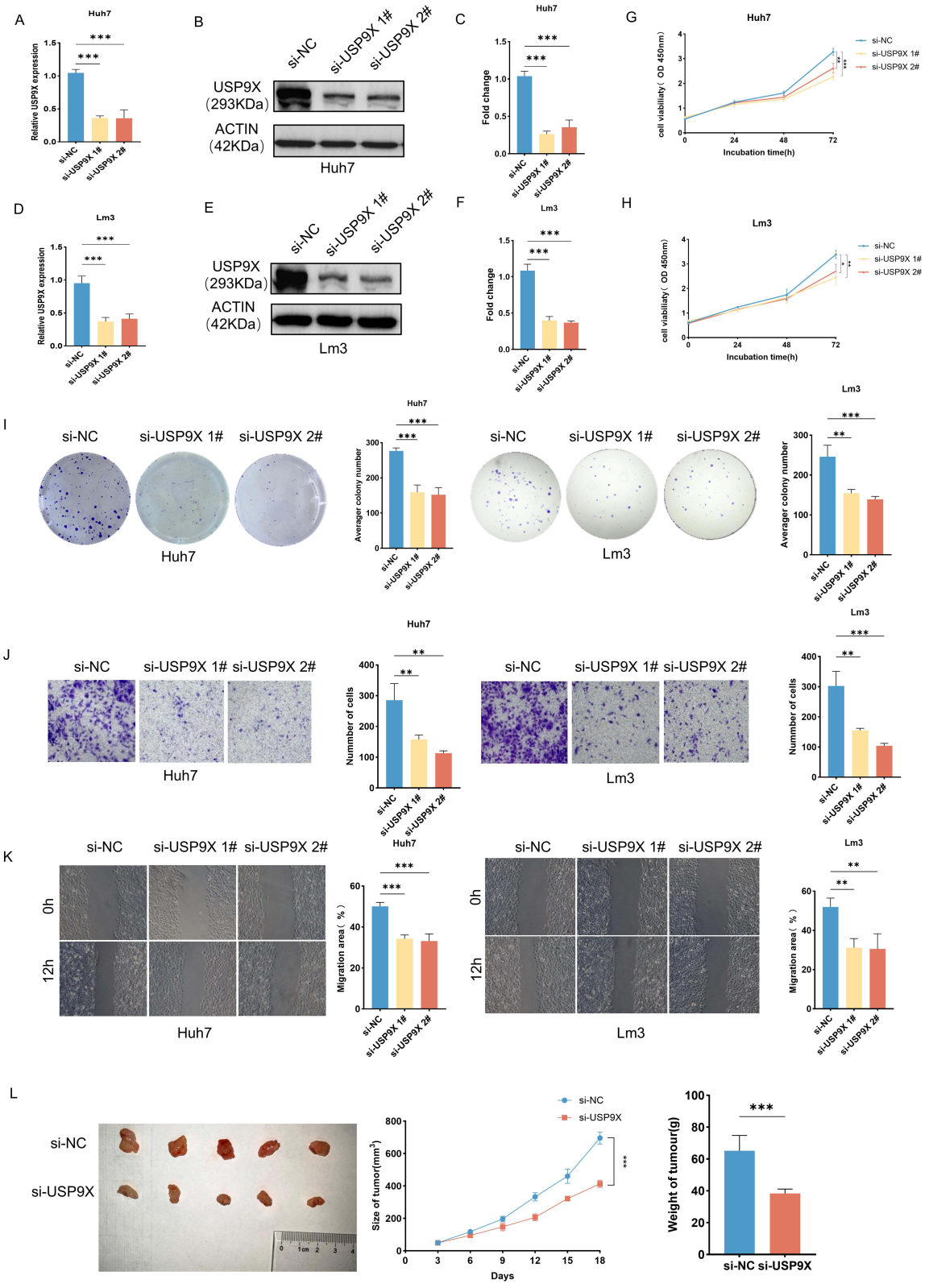

Figure 3 Knockdown of USP9X suppresses HCC cell proliferation and tumorigenicity. (**A**–**F**) qRT-PCR and Western blot validation showing that two siRNAs (si-USP9X #1 and si-USP9X #2) efficiently reduced USP9X mRNA and protein expression in Huh7 and Lm3 cells. (**G** and **H**) CCK-8 assays showing that USP9X knockdown markedly inhibited proliferation of (**G**) Huh7 and (**H**) Lm3 cells compared with si-NC controls. (**I**) Colony formation assays showing that USP9X depletion significantly decreased clonogenic capacity ($P < 0.001$). (**J**) Transwell assays demonstrating that USP9X silencing reduced migration and invasion in both Huh7 and Lm3 cells ($P < 0.01$, $P < 0.001$). (**K**) Wound-healing assays further confirming impaired migration after USP9X knockdown ($P < 0.01$, $P < 0.001$). (**L**) In vivo xenograft experiments showing that USP9X knockdown significantly inhibited tumor growth rate and final tumor weight (*$P < 0.05$, **$P < 0.01$, ***$P < 0.001$).

https://doi.org/10.2147/JHC.S585217

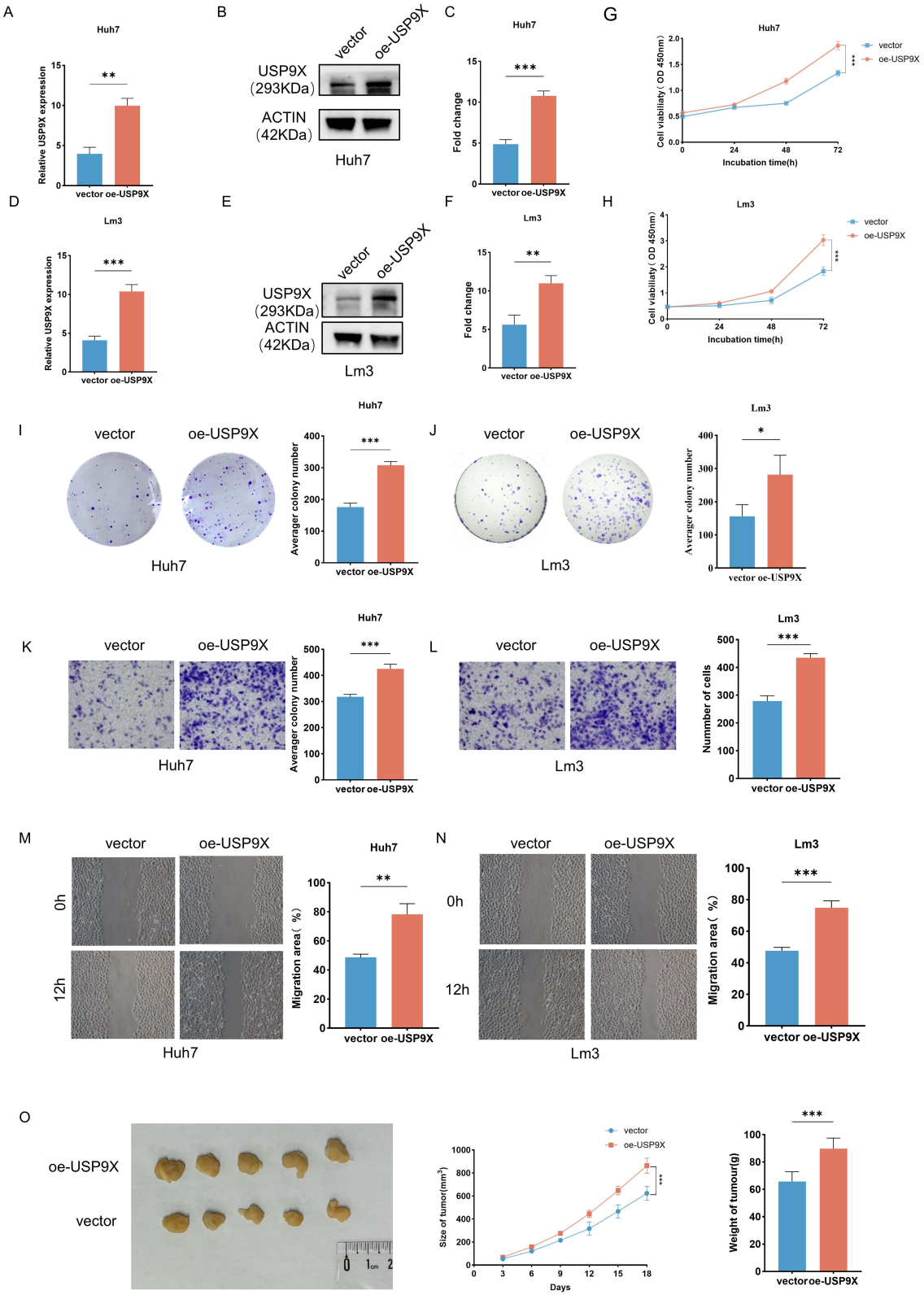

Figure 4 Overexpression of USP9X promotes HCC cell proliferation and tumor growth. (**A**–**F**) qRT-PCR and Western blot validation showing that the overexpression plasmid (oe-USP9X) effectively increased USP9X mRNA and protein levels in Huh7 and Lm3 cells. (**G** and **H**) CCK-8 assays indicating that USP9X overexpression significantly enhanced proliferation of (**G**) Huh7 and (**H**) Lm3 cells compared with vector controls. (**I** and **J**) Colony formation assays showing that USP9X overexpression significantly increased colony numbers in (**I**) Huh7 and (**J**) Lm3 cells ($P < 0.05$, $P < 0.001$). (**K** and **L**) Transwell assays showing that USP9X overexpression enhanced migration and invasion in (**K**) Huh7 and (**L**) Lm3 cells ($P < 0.001$). (**M** and **N**) Wound-healing assays confirming that USP9X overexpression accelerated wound closure in (**M**) Huh7 and (**N**) Lm3 cells. (**O**) In vivo xenograft assays showing that USP9X overexpression significantly increased tumor growth rate and final tumor weight (*$P < 0.05$, **$P < 0.01$, ***$P < 0.001$).

https://doi.org/10.2147/JHC.S585217

Table 1 LC-MS Analysis of USP9X Complexes: Top 10 Hits Ranked by Search Score

Gene Names	USP9X	HSP90AA1	TNRC6B	UBA1	LDHB	UBR4	NACA	FSCN1	PDIA3
Score	203.71	105.67	68.51	55.94	55.29	54.84	52.514	51.021	48.551

xenograft models, USP9X-overexpressing cells formed significantly larger and heavier tumors than controls (n = 5 mice per group, Figure 4O), confirming the tumor-promoting role of USP9X in vivo.

USP9X Stabilizes HSP90AA1 to Promote Its Upregulation in HCC and Associates with Poor Prognosis

Co-immunoprecipitation followed by mass spectrometry identified HSP90AA1 as a potential USP9X-interacting protein (Table 1). Overexpression of USP9X markedly increased HSP90AA1 protein levels, while USP9X knockdown decreased them (Figure 5A and B). TCGA-LIHC data confirmed significantly elevated HSP90AA1 expression in tumors compared with normal liver tissue (Figure 5C), and high HSP90AA1 expression correlated with poor overall survival (Figure 5D). A strong positive correlation was observed between USP9X and HSP90AA1 transcript levels ($R = 0.46$, $P = 3.5 \times 10^{-29}$) (Figure 5E). Cycloheximide chase assays showed that USP9X depletion accelerated HSP90AA1 degradation, while USP9X overexpression prolonged its stability (Figure 5F and G). Treatment with the proteasome inhibitor MG132 restored HSP90AA1 levels suppressed by USP9X knockdown (Figure 5H), indicating that USP9X stabilizes HSP90AA1 by preventing proteasomal degradation. Together, these data identify USP9X as a critical deubiquitinase that stabilizes HSP90AA1, with both proteins co-upregulated in HCC and associated with adverse prognosis.

USP9X Directly Binds and Deubiquitinates HSP90AA1

Endogenous co-immunoprecipitation (Co-IP) assays using anti-USP9X and anti-HSP90AA1 antibodies confirmed reciprocal binding between the two proteins in Huh7 and Lm3 cells, with no interaction observed in IgG controls (Figure 6A and B). Co-expression of Flag-USP9X and Myc-HSP90AA1 in HEK293 cells confirmed a direct interaction (Figure 6C and D). Deubiquitination assays in the presence of MG132 revealed that USP9X overexpression markedly reduced Myc-HSP90AA1 ubiquitination (Figure 6E). Linkage-specific analyses demonstrated that USP9X preferentially removed K48-linked polyubiquitin chains, with minimal effect on K63-linked chains (Figure 6F). These findings demonstrate that USP9X directly binds to HSP90AA1 and removes K48-linked polyubiquitin chains to antagonize proteasomal degradation and enhance protein stability.

USP9X Promotes HCC Malignancy by Stabilizing HSP90AA1, Its Key Downstream Effector

Rescue experiments were conducted to verify whether HSP90AA1 mediates the oncogenic effects of USP9X in HCC. Western blotting in Huh7 and Lm3 cells showed that USP9X knockdown reduced HSP90AA1 protein expression, which was restored by exogenous HSP90AA1 overexpression, whereas HSP90AA1 silencing reversed the upregulation induced by USP9X overexpression (Figure 7A and B). Functionally, CCK-8 assays demonstrated that HSP90AA1 restoration rescued the inhibitory effect of USP9X depletion on cell viability, while HSP90AA1 knockdown attenuated USP9X-driven proliferation (Figure 7C and D). Similar trends were observed in colony formation, Transwell, and wound-healing assays, indicating that HSP90AA1 is required for USP9X-mediated enhancement of clonogenicity and migration (Figure 7E; sfigure 1A and B). In xenograft models, re-expression of HSP90AA1 restored tumor growth suppressed by USP9X silencing, whereas HSP90AA1 depletion blunted the tumor-promoting effect of USP9X overexpression (n = 5 mice per group, Figure 7F). Together, these findings indicate that USP9X exerts its oncogenic role in HCC, at least in part, through HSP90AA1.

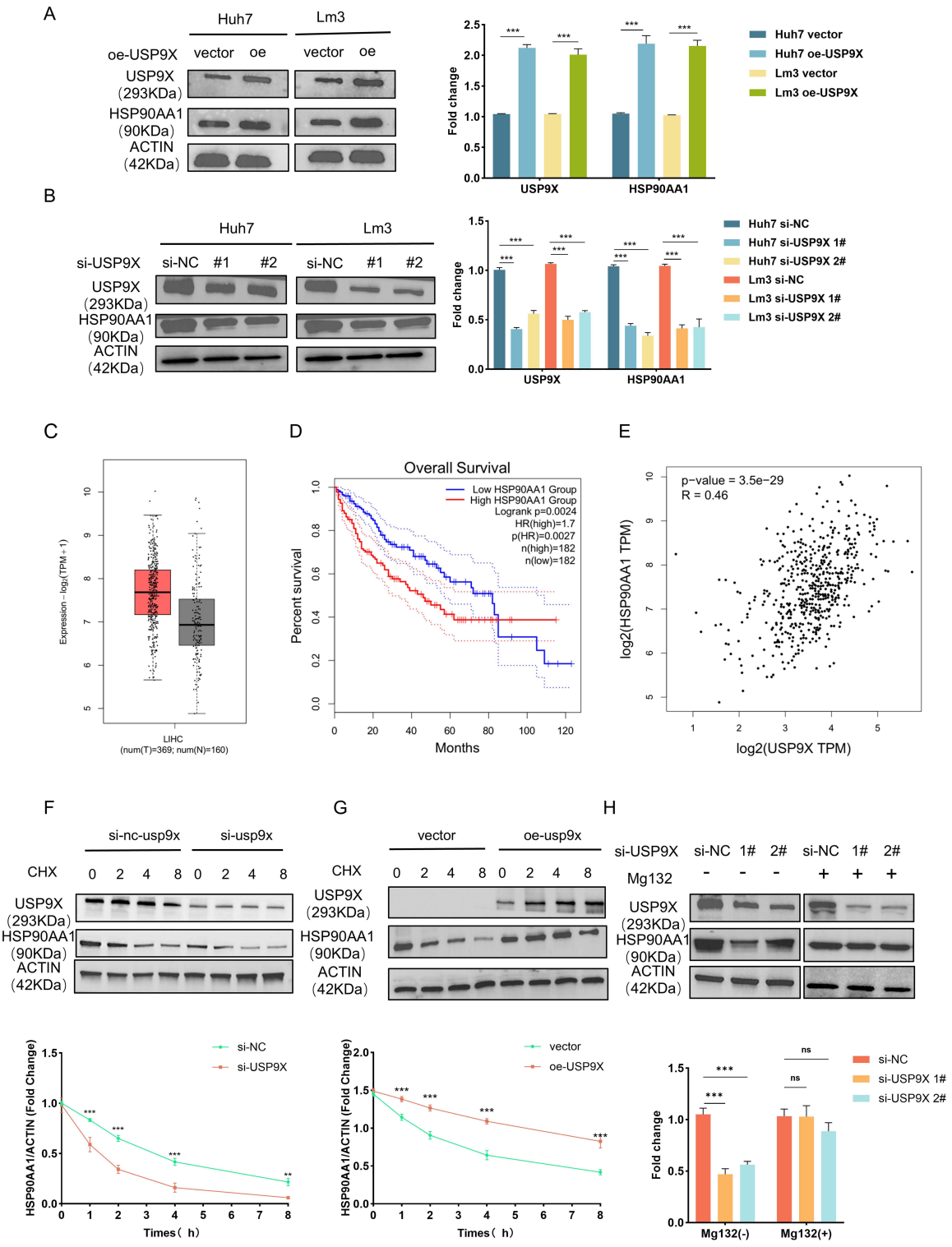

Figure 5 USP9X stabilizes HSP90AA1, promoting its upregulation in HCC and correlating with poor prognosis. (**A** and **B**) Western blot analysis showing that USP9X overexpression (oe-USP9X) increased, while USP9X knockdown (si-USP9X) decreased HSP90AA1 protein levels in Huh7 and Lm3 cells. (**C**–**E**) TCGA analysis showing that HSP90AA1 expression was significantly higher in HCC tissues (red box) than in normal liver tissues (black box). High HSP90AA1 expression correlates with worse overall survival (HR = 1.7, P = 0.002) and positively correlates with USP9X expression (R = 0.46, P < 0.01). (**F**–**G**) Cycloheximide (CHX) chase assays showing that USP9X silencing accelerated HSP90AA1 degradation, whereas USP9X overexpression prolonged its stability. (**H**) Treatment with the proteasome inhibitor MG132 rescued HSP90AA1 degradation induced by USP9X knockdown, indicating that USP9X stabilizes HSP90AA1 by preventing proteasome-mediated degradation (**P < 0.01, ***P < 0.001, ns: not significant. The presence (+) or absence (–) of the indicated treatments is shown above.).

https://doi.org/10.2147/JHC.S585217

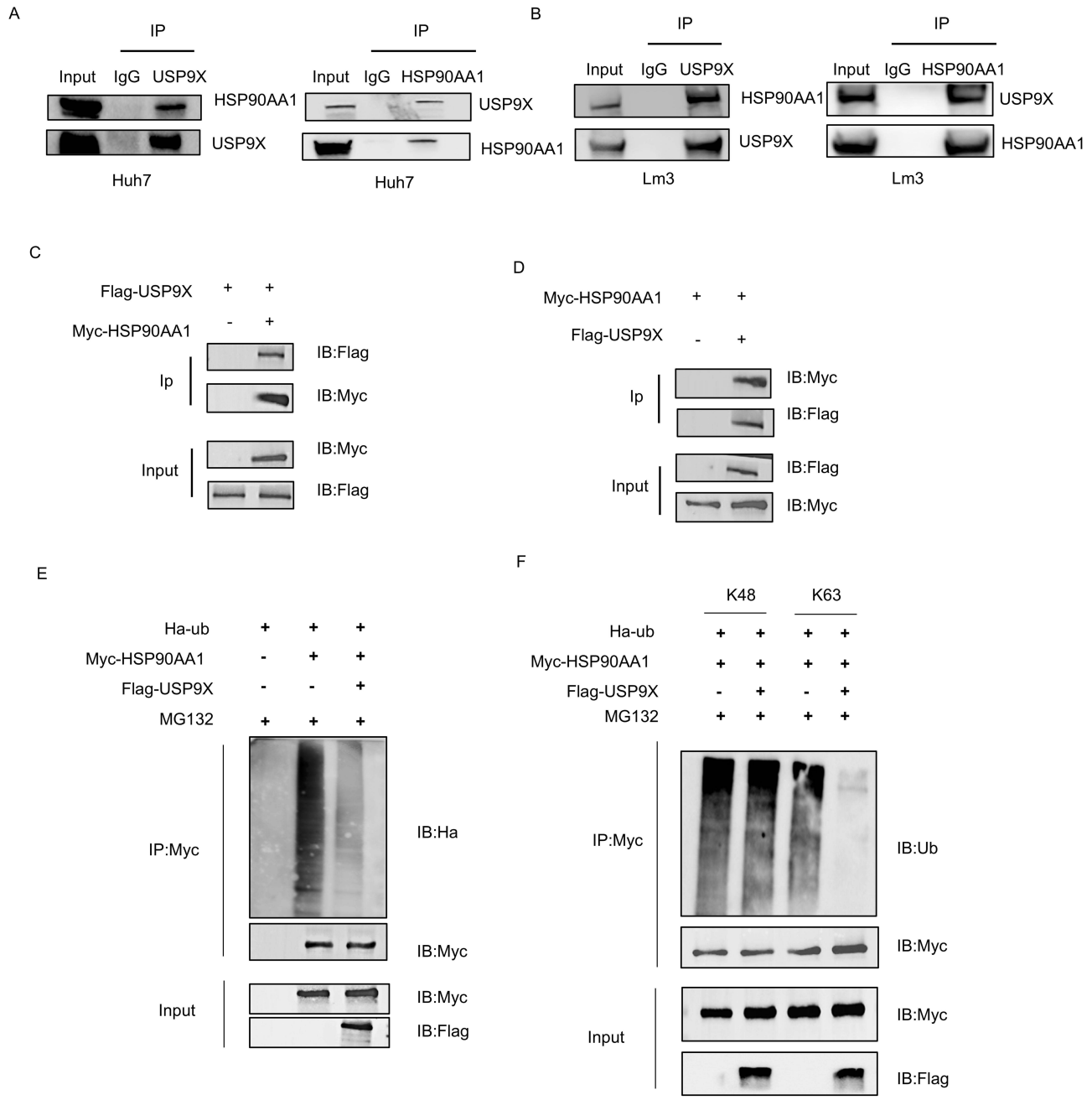

Figure 6 USP9X directly binds to and deubiquitinates HSP90AA1. (**A** and **B**) Endogenous co-immunoprecipitation (Co-IP) assays confirming the interaction between USP9X and HSP90AA1 in Huh7 and Lm3 cells. (**C** and **D**) Exogenous Co-IP assays verifying the direct interaction between Flag-USP9X and Myc-HSP90AA1. (**E** and **F**) In vivo ubiquitination assays demonstrating that USP9X removes ubiquitin modifications from HSP90AA1, preferentially targeting K48-linked polyubiquitin chains. (Plus sign (+) indicates that the corresponding reagent (eg, Flag-USP9X, MG132, K48-linked ubiquitin) was added or expressed; minus sign (–) indicates the control without that reagent.).

Discussion

Hepatocellular carcinoma (HCC) remains one of the most prevalent and lethal malignancies worldwide, with persistently poor survival outcomes. According to the World Health Organization, over one million deaths from HCC are projected to occur by 2030.[39] Identifying novel therapeutic targets to improve patient prognosis is therefore a major clinical priority. Deubiquitination, a central process within the protein homeostasis network, regulates protein stability, activity, and localization by removing ubiquitin chains from substrate proteins. Through this mechanism, deubiquitinating enzymes (DUBs) exert precise control over cellular fate.[40] Dysregulation of DUBs disturbs the balance of key tumor suppressors and oncogenic proteins—such as PTEN and Snail—thereby promoting cancer progression, invasion, and metastasis.[15]

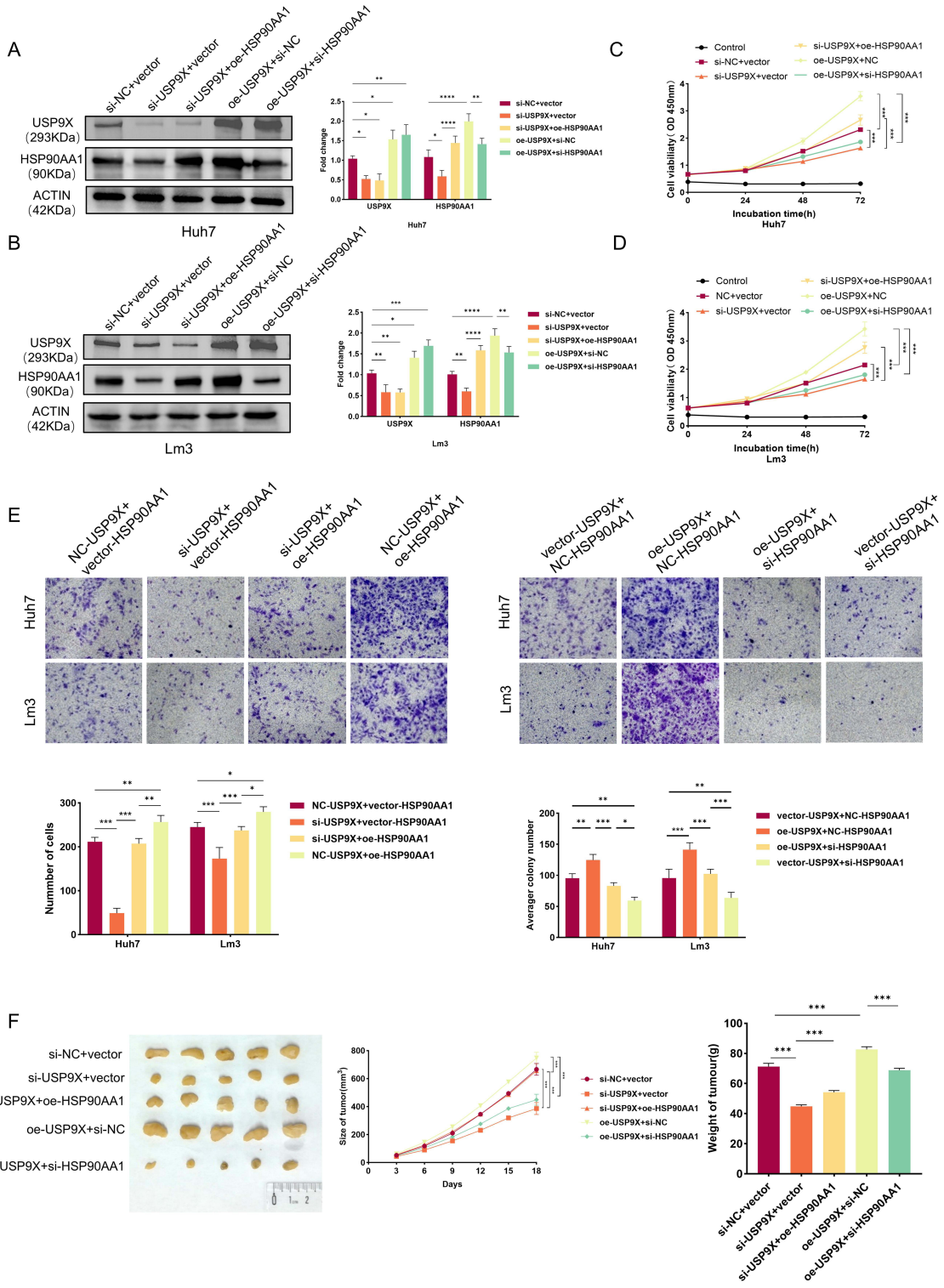

Figure 7 USP9X promotes HCC malignancy by stabilizing HSP90AA1, which acts as a key downstream effector. (**A** and **B**) Western blot and quantitative analyses showing that USP9X knockdown decreased HSP90AA1 protein levels in Huh7 (**A**) and Lm3 (**B**) cells, which were restored by HSP90AA1 overexpression. Conversely, USP9X overexpression increased HSP90AA1 levels, while co-silencing HSP90AA1 abrogated this effect. (**C** and **D**) CCK-8 proliferation curves showing that USP9X knockdown inhibited 0–72 h cell growth, rescued by HSP90AA1 reintroduction; USP9X overexpression enhanced proliferation, which was weakened by HSP90AA1 knockdown (Huh7: (**C**); Lm3: (**D**)). (**E**) Transwell assays showing that USP9X knockdown reduced migration, rescued by HSP90AA1 overexpression; USP9X overexpression enhanced migration, which was suppressed by HSP90AA1 knockdown. (**F**) In vivo xenograft experiments showing representative tumor images, tumor growth curves, and final tumor weights: USP9X knockdown suppressed tumor growth, rescued by HSP90AA1 overexpression; USP9X overexpression enhanced tumorigenicity, which was significantly reduced upon HSP90AA1 silencing (*P < 0.05, **P < 0.01, ***P < 0.001, **** P < 0.0001).

https://doi.org/10.2147/JHC.S585217

Given their substrate specificity and reversible enzymatic nature, DUBs have attracted increasing attention as potential therapeutic targets in cancer.[41]

In this study, we identify a novel oncogenic mechanism in which USP9X, a member of the ubiquitin-specific protease family, drives HCC progression by stabilizing HSP90AA1 through deubiquitination. We demonstrate that USP9X expression is markedly upregulated in HCC and correlates with unfavorable clinical outcomes. Functional analyses show that USP9X promotes tumor cell proliferation, colony formation, migration, invasion, and xenograft tumor growth. Mechanistically, USP9X directly binds to HSP90AA1 and removes K48-linked polyubiquitin chains, preventing proteasome-mediated degradation and enhancing HSP90AA1 stability. Collectively, these findings define the USP9X–HSP90AA1 signaling axis as a key driver of HCC malignancy and a promising therapeutic target.

The biological role of USP9X in cancer is highly context-dependent.[42] Elevated USP9X expression has been reported in multiple tumor types, including pancreatic, esophageal, and glioblastoma cancers,[24,43,44] where it promotes oncogenic signaling and tumor progression. In contrast, in other malignancies such as cholangiocarcinoma, USP9X exerts tumor-suppressive effects by stabilizing distinct substrates.[26] Our findings reinforce the oncogenic nature of USP9X in HCC and reveal a previously unrecognized downstream mechanism. Prior studies have shown that USP9X facilitates HCC progression by stabilizing β-catenin; however, our results identify HSP90AA1 as an alternative and novel substrate. Moreover, while HSP90AA1 stability is known to be regulated by FBXL6-mediated ubiquitination[33] and USP14-mediated deubiquitination,[45] both of which influence liver disease progression, our study introduces USP9X as a new deubiquitinase for HSP90AA1. This discovery expands the regulatory network governing HSP90AA1 stability and identifies USP9X as a distinct, functionally important component of this pathway.

HSP90AA1, a major cytoplasmic chaperone, performs multifaceted roles in cancer biology.[46] Beyond its canonical chaperone activity, HSP90AA1 regulates transcriptional processes[47] and modulates autophagy. Under basal conditions, phosphorylation of HSP90AA1 by CDK5 at Ser595 inhibits its interaction with transcription factor EB (TFEB), thereby preventing TFEB nuclear localization and autophagy activation.[48] This mechanism is functionally aligned with the well-established PI3K/AKT/mTOR signaling pathway, which also critically regulates autophagy in cancer cells by phosphorylating and cytoplasmic retention of TFEB through mTORC1.[49,50] Furthermore, HSP90AA1-mediated autophagy contributes to chemoresistance; in osteosarcoma cells, HSP90AA1 enhances autophagy through the PI3K/Akt/mTOR pathway while suppressing apoptosis via JNK/P38 signaling.[51] In HCC, nuclear HSP90AA1 interacts with host cell factor 1 (HCFC1) to occupy the TFEB promoter, maintaining TFEB transcriptional activity and nuclear localization. This leads to upregulation of LC3 and p62, sustaining autophagy–lysosomal gene expression essential for mitochondrial quality control (MQC).[48,51]

These observations suggest that USP9X-mediated stabilization of HSP90AA1 may contribute not only to tumor growth, but also to autophagic regulation and metabolic adaptation in HCC. Previous studies have shown that USP9X promotes autophagy and drug resistance in HCC through stabilization of p53.[52] Our findings extend this model by identifying HSP90AA1 as an additional downstream effector through which USP9X drives malignant progression. We therefore speculate that the USP9X–HSP90AA1 axis may orchestrate a broader proteostatic and metabolic program involving autophagy- and stress-response pathways, thereby enhancing tumor cell survival under adverse conditions. Further investigation of these downstream events will help clarify the molecular basis by which HCC sustains adaptive resilience. From a translational perspective, the upregulation of USP9X in HCC tissues and its association with poor prognosis indicate that USP9X may have value not only as a functional oncogenic driver, but also as a potential prognostic biomarker. Evaluation of USP9X expression may assist in identifying patients with more aggressive disease and improve risk stratification for individualized clinical management.

Despite the robustness of our data, several limitations should be acknowledged. First, this study primarily focuses on the direct interaction between USP9X and HSP90AA1, while the global signaling network affected by HSP90AA1 stabilization remains incompletely characterized. Second, potential cofactors or interacting partners of USP9X and HSP90AA1 were not investigated. Third, the lack of selective inhibitors targeting the USP9X–HSP90AA1 interaction currently limits immediate translational application.

Future research should therefore pursue three directions: (1) Systematic identification of HSP90AA1 client proteins in HCC using quantitative proteomics and interactome mapping; (2) Development or screening of small-molecule inhibitors

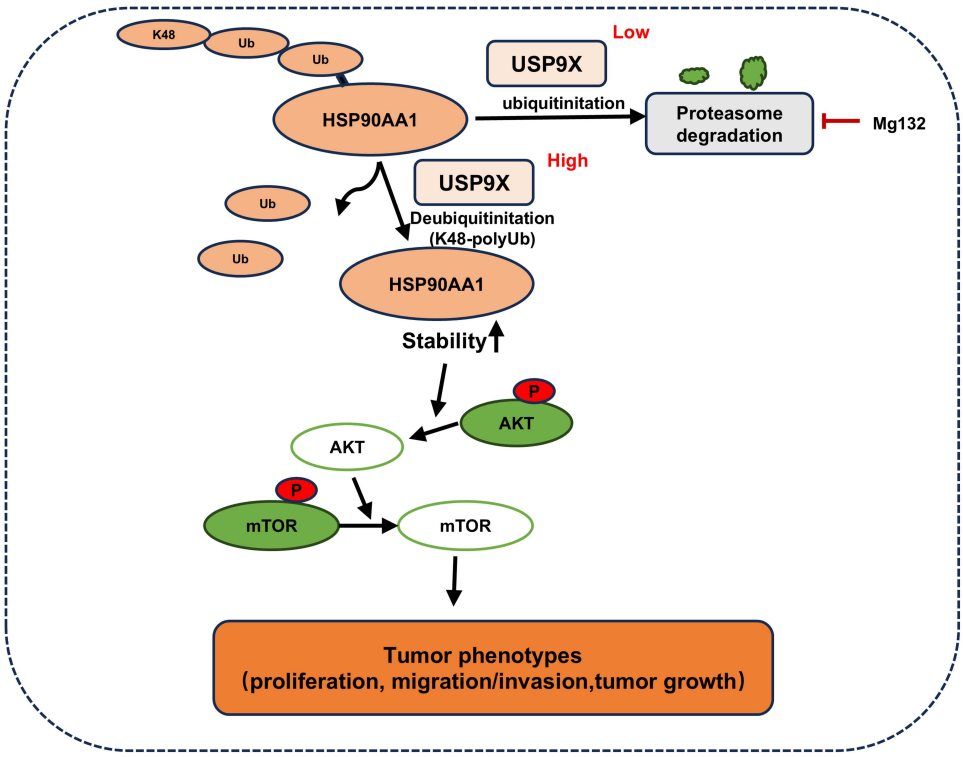

Figure 8 USP9X deubiquitinates and stabilizes HSP90AA1, activating the HCFC1/TFEB autophagy–lysosome program to promote tumor progression. (Upward arrows indicate positive regulation or enhancement of the corresponding process or protein level).

that selectively disrupt the USP9X–HSP90AA1 interaction; (3) Validation of this pathway's therapeutic relevance in physiologically representative orthotopic HCC models, assessing its effects on tumor growth, metastasis, and drug responsiveness.

In conclusion, this study identifies USP9X as a critical deubiquitinase of HSP90AA1 and elucidates the USP9X–HSP90AA1 axis as a novel molecular mechanism promoting HCC malignancy (Figure 8). These findings expand the understanding of deubiquitination-mediated proteostasis in liver cancer and provide a theoretical and experimental foundation for developing USP9X-based prognostic tools and therapeutic strategies in HCC.

Data Sharing Statement

The data that support the findings of this study are avail able in the methods and results sections of this article.

Ethics Approval and Informed Consent

All human samples were obtained with informed consent from patients with liver cancer. Ethical consent was granted from the Ethical Committee Review Board of the Affiliated Suzhou Hospital of Nanjing Medical University (No. KL901605). The animal study was reviewed and approved by the Institutional Animal Care and Use Committee (IACUC) of the Suzhou Institute of Systems Medicine (ISM) (permit number: ISM-IACUC-20250146).

Acknowledgments

This work was supported by Suzhou Clinical Medical Center Construction Project (Szlcyxzxj202107), Suzhou City "Science and Education Promoting Health" Youth Science and Technology Project (KJXW2023040), Suzhou Basic Research Program (Medical Application Basic Research)(SKYD2023141), Suzhou City Applied Basic Research (Medical and Health) Technology Innovation Project (SYW2024028) and Suzhou City Applied Basic Research (Medical and Health) Technology Innovation Project (SKY2022192).

Disclosure

The authors declare that they have no known competing financial interests or personal relationships that could have appeared to influence the work reported in this paper.

References

1. Bray F, Laversanne M, Sung H, et al. Global cancer statistics 2022: GLOBOCAN estimates of incidence and mortality worldwide for 36 cancers in 185 countries. *Ca a Cancer J Clin*. 2024;3:229–263. doi:10.3322/caac.21834
2. Rumgay H, Arnold M, Ferlay J, et al. Global burden of primary liver cancer in 2020 and predictions to 2040. *J Hepatol*. 2022;6(6):1598–1606. doi:10.1016/j.jhep.2022.08.021
3. Tan EY, Danpanichkul P, Yong JN, et al. Liver cancer in 2021: global burden of disease study. *J Hepatol*. 2025;5(5):851–860. doi:10.1016/j.jhep.2024.10.031
4. Arnold M, Abnet CC, Neale RE, et al. Global burden of 5 major types of gastrointestinal cancer. *Gastroenterology*. 2020;1(1):335–349.e315. doi:10.1053/j.gastro.2020.02.068
5. Department of Medical Administration NHCotPsRoC. Guidelines for the diagnosis and treatment of primary liver cancer (2026 edition). *China J General Surg*. 2026;4:1–71. doi:10.7659/j.issn.1005-6947.260031
6. Siegel RL, Kratzer TB, Wagle NS, Sung H, Jemal A. Cancer statistics, 2026. *CA Cancer J Clin*. 2026;1:e70043. doi:10.3322/caac.70043
7. Man XB, Tang L, Zhang BH, et al. Upregulation of Glypican-3 expression in hepatocellular carcinoma but downregulation in cholangiocarcinoma indicates its differential diagnosis value in primary liver cancers. *Liver Int*. 2005;5(5):962–966. doi:10.1111/j.1478-3231.2005.01100.x
8. Shen Q, Fan J, Yang XR, et al. Serum DKK1 as a protein biomarker for the diagnosis of hepatocellular carcinoma: a large-scale, multicentre study. *Lancet Oncol*. 2012;8(8):817–826. doi:10.1016/s1470-2045(12)70233-4
9. Lim KC, Chow PK, Allen JC, Siddiqui FJ, Chan ES, Tan SB. Systematic review of outcomes of liver resection for early hepatocellular carcinoma within the Milan criteria. *Br J Surg*. 2012;12(12):1622–1629. doi:10.1002/bjs.8915
10. Straś WA, Wasiak D, Łągiewska B, et al. Recurrence of hepatocellular carcinoma after liver transplantation: risk factors and predictive models. *Ann Transplant*. 2022;27:e934924. doi:10.12659/aot.934924
11. Shah SA, Cleary SP, Wei AC, et al. Recurrence after liver resection for hepatocellular carcinoma: risk factors, treatment, and outcomes. *Surgery*. 2007;3(3):330–339. doi:10.1016/j.surg.2006.06.028
12. Roayaie S, Schwartz JD, Sung MW, et al. Recurrence of hepatocellular carcinoma after liver transplant: patterns and prognosis. *Liver Transplant*. 2004;4(4):534–540. doi:10.1002/lt.20128
13. Utsunomiya T, Shimada M, Imura S, Morine Y, Ikemoto T, Mori M. Molecular signatures of noncancerous liver tissue can predict the risk for late recurrence of hepatocellular carcinoma. *J Gastroenterol*. 2010;2(2):146–152. doi:10.1007/s00535-009-0164-1
14. Li L, Wang H. Heterogeneity of liver cancer and personalized therapy. *Cancer Lett*. 2016;2(2):191–197. doi:10.1016/j.canlet.2015.07.018
15. Balch WE, Morimoto RI, Dillin A, Kelly JW. Adapting proteostasis for disease intervention. *Science*. 2008;5865(5865):916–919. doi:10.1126/science.1141448
16. Bett JS. Proteostasis regulation by the ubiquitin system. *Essays Biochem*. 2016;2:143–151. doi:10.1042/ebc20160001
17. Liu F, Chen J, Li K, et al. Ubiquitination and deubiquitination in cancer: from mechanisms to novel therapeutic approaches. *Mol Cancer*. 2024;1:148. doi:10.1186/s12943-024-02046-3
18. Cockram PE, Kist M, Prakash S, Chen SH, Wertz IE, Vucic D. Ubiquitination in the regulation of inflammatory cell death and cancer. *Cell Death Differ*. 2021;2(2):591–605. doi:10.1038/s41418-020-00708-5
19. Tian Z, Xu C, He W, et al. The deubiquitinating enzyme USP19 facilitates hepatocellular carcinoma progression through stabilizing YAP. *Cancer Lett*. 2023;577:216439. doi:10.1016/j.canlet.2023.216439
20. Lv XY, Duan T, Li J. The multiple roles of deubiquitinases in liver cancer. *Am J Cancer Res*. 2020;6:1647–1657.
21. Gao H, Chen Z, Zhao L, Ji C, Xing F. Cellular functions, molecular signalings and therapeutic applications: translational potential of deubiquitylating enzyme USP9X as a drug target in cancer treatment. *Biochim Biophys Acta Rev Cancer*. 2024;3(3):189099. doi:10.1016/j.bbcan.2024.189099
22. Wang P, Wang J, Yao S, et al. Deubiquitinase USP9X stabilizes RNA m(6)A demethylase ALKBH5 and promotes acute myeloid leukemia cell survival. *J Biol Chem*. 2023;8(8):105055. doi:10.1016/j.jbc.2023.105055
23. Chen Y, Feng X, Wu Z, et al. USP9X-mediated REV1 deubiquitination promotes lung cancer radioresistance via the action of REV1 as a Rad18 molecular scaffold for cystathionine gamma-lyase. *J Biomed Sci*. 2024;1(1):55. doi:10.1186/s12929-024-01044-3
24. Perurena N, Lock R, Davis RA, et al. USP9X mediates an acute adaptive response to MAPK suppression in pancreatic cancer but creates multiple actionable therapeutic vulnerabilities. *Cell Rep Med*. 2023;4(4):101007. doi:10.1016/j.xcrm.2023.101007
25. Golla C, Bilal M, Dwucet A, et al. Photodynamic therapy combined with Bcl-2/Bcl-xL inhibition increases the Noxa/Mcl-1 ratio independent of Usp9X and synergistically enhances apoptosis in glioblastoma. *Cancers*. 2021;16(16):4123. doi:10.3390/cancers13164123
26. Chen W, Song J, Liu S, et al. USP9X promotes apoptosis in cholangiocarcinoma by modulation expression of KIF1Bbeta via deubiquitinating EGLN3. *J Biomed Sci*. 2021;1(1):44. doi:10.1186/s12929-021-00738-2
27. Calderwood SK, Khaleque MA, Sawyer DB, Ciocca DR. Heat shock proteins in cancer: chaperones of tumorigenesis. *Trends Biochem Sci*. 2006;3(3):164–172. doi:10.1016/j.tibs.2006.01.006
28. Wang C, Zhang Y, Guo K, et al. Heat shock proteins in hepatocellular carcinoma: molecular mechanism and therapeutic potential. *Int J Cancer*. 2016;8(8):1824–1834. doi:10.1002/ijc.29723
29. Staufer K, Stoeltzing O. Implication of heat shock protein 90 (HSP90) in tumor angiogenesis: a molecular target for anti-angiogenic therapy? *Curr Cancer Drug Targets*. 2010;8(8):890–897. doi:10.2174/156800910793357934
30. Xu Q, Tu J, Dou C, et al. HSP90 promotes cell glycolysis, proliferation and inhibits apoptosis by regulating PKM2 abundance via Thr-328 phosphorylation in hepatocellular carcinoma. *Mol Cancer*. 2017;1(1):178. doi:10.1186/s12943-017-0748-y
31. Chu SH, Liu YW, Zhang L, et al. Regulation of survival and chemoresistance by HSP90AA1 in ovarian cancer SKOV3 cells. *Molecular Biology Reports*. 2013;1(1):1–6. doi:10.1007/s11033-012-1930-3

32. Gao J, Aksoy BA, Dogrusoz U, et al. Integrative analysis of complex cancer genomics and clinical profiles using the cBioPortal. *Sci Signaling*. 2013;269:11. doi:10.1126/scisignal.2004088
33. Shi W, Feng L, Dong S, et al. FBXL6 governs c-MYC to promote hepatocellular carcinoma through ubiquitination and stabilization of HSP90AA1. *Cell Commun Signal*. 2020;1(1):100. doi:10.1186/s12964-020-00604-y
34. Khandelwal A, Crowley VM, Blagg BSJ. Natural product inspired N-terminal Hsp90 inhibitors: from bench to bedside? *Med Res Rev*. 2016;1(1):92–118. doi:10.1002/med.21351
35. Zhao Y, Qin J, Yu D, et al. Polymer-locking fusogenic liposomes for glioblastoma-targeted siRNA delivery and CRISPR-Cas gene editing. *Nature Nanotechnol*. 2024;12(12):1869–1879. doi:10.1038/s41565-024-01769-0
36. Li Z, Meng X, Wu P, et al. Glioblastoma cell-derived lncRNA-containing exosomes induce microglia to produce complement C5, promoting chemotherapy resistance. *Cancer Immunol Res*. 2021;12(12):1383–1399. doi:10.1158/2326-6066.Cir-21-0258
37. Zhang Z, Wang Z, Huang K, et al. PLK4 is a determinant of temozolomide sensitivity through phosphorylation of IKBKE in glioblastoma. *Cancer Lett*. 2019;443:91–107. doi:10.1016/j.canlet.2018.11.034
38. Zhang FK, Ni QZ, Wang K, et al. Targeting USP9X-AMPK axis in ARID1A-deficient hepatocellular carcinoma. *Cell Mol Gastroenterol Hepatol*. 2022;1(1):101–127. doi:10.1016/j.jcmgh.2022.03.009
39. Sung H, Ferlay J, Siegel RL, et al. Global cancer statistics 2020: GLOBOCAN estimates of incidence and mortality worldwide for 36 cancers in 185 countries. *CA Cancer J Clin*. 2021;3:209–249. doi:10.3322/caac.21660
40. Millán-Zambrano G, Burton A, Bannister AJ, Schneider R. Histone post-translational modifications - cause and consequence of genome function. *Nat Rev Genet*. 2022;9(9):563–580. doi:10.1038/s41576-022-00468-7
41. Han S, Wang R, Zhang Y, et al. The role of ubiquitination and deubiquitination in tumor invasion and metastasis. *Int J Bio Sci*. 2022;6(6):2292–2303. doi:10.7150/ijbs.69411
42. Hu M, Li P, Li M, et al. Crystal structure of a UBP-family deubiquitinating enzyme in isolation and in complex with ubiquitin aldehyde. *Cell*. 2002;7(7):1041–1054. doi:10.1016/s0092-8674(02)01199-6
43. Wei B, Xu L, Hui H, Sun Y, Wu J. USP9X mRNA expression predicts clinical outcome for esophageal squamous cell carcinoma treated with cisplatin-based therapy. *Clin Res Hepatol Gastroenterol*. 2020;6(6):932–938. doi:10.1016/j.clinre.2019.10.004
44. Chen Z, Wang HW, Wang S, et al. USP9X deubiquitinates ALDH1A3 and maintains mesenchymal identity in glioblastoma stem cells. *J Clin Invest*. 2019;5(5):2043–2055. doi:10.1172/JCI126414
45. Wei D, Tian X, Zhu L, Wang H, Sun C. USP14 governs CYP2E1 to promote nonalcoholic fatty liver disease through deubiquitination and stabilization of HSP90AA1. *Cell Death Dis*. 2023;8(8):566. doi:10.1038/s41419-023-06091-6
46. Picard D. Heat-shock protein 90, a chaperone for folding and regulation. *Cell Mol Life Sci*. 2002;10(10):1640–1648. doi:10.1007/pl00012491
47. Khurana N, Bhattacharyya S. Hsp90, the concertmaster: tuning transcription. *Front Oncol*. 2015;5:100. doi:10.3389/fonc.2015.00100
48. Yang S, Nie T, She H, et al. Regulation of TFEB nuclear localization by HSP90AA1 promotes autophagy and longevity. *Autophagy*. 2023;3(3):822–838. doi:10.1080/15548627.2022.2105561
49. Janku F, McConkey DJ, Hong DS, Kurzrock R. Autophagy as a target for anticancer therapy. *Nat Rev Clin Oncol*. 2011;9(9):528–539. doi:10.1038/nrclinonc.2011.71
50. Settembre C, Zoncu R, Medina DL, et al. A lysosome-to-nucleus signalling mechanism senses and regulates the lysosome via mTOR and TFEB. *EMBO J*. 2012;5(5):1095–1108. doi:10.1038/emboj.2012.32
51. Xiao X, Wang W, Li Y, et al. HSP90AA1-mediated autophagy promotes drug resistance in osteosarcoma. *J Experiment Clin Cancer Res*. 2018;1(1):201. doi:10.1186/s13046-018-0880-6
52. Chen E, Li E, Liu H, et al. miR-26b enhances the sensitivity of hepatocellular carcinoma to Doxorubicin via USP9X-dependent degradation of p53 and regulation of autophagy. *Int J Biol Sci*. 2021;3(3):781–795. doi:10.7150/ijbs.52517